Video Article

In vivo Measurement of the Mouse Pulmonary Endothelial Surface Layer

Yimu Yang, Gaoqing Yang, Eric P. Schmidt

Division of Pulmonary Sciences and Critical Care Medicine, University of Colorado School of Medicine

Correspondence to: Eric P. Schmidt at eric.schmidt@ucdenver.edu

URL: http://www.jove.com/video/50322
DOI: doi:10.3791/50322

Keywords: Medicine, Issue 72, Cellular Biology, Anatomy, Physiology, Biomedical Engineering, Biophysics, Surgery, Endothelium, Vascular, Inflammation, Pulmonary Circulation, Intravital Microscopy, endothelial surface layer, endothelial, glycocalyx, pulmonary microvasculature, catheter, tracheostomy, venous, catheterization, lung injury, mouse, animal model

Date Published: 2/22/2013

Citation: Yang, Y., Yang, G., Schmidt, E.P. *In vivo* Measurement of the Mouse Pulmonary Endothelial Surface Layer. *J. Vis. Exp.* (72), e50322, doi:10.3791/50322 (2013).

Abstract

The endothelial glycocalyx is a layer of proteoglycans and associated glycosaminoglycans lining the vascular lumen. *In vivo*, the glycocalyx is highly hydrated, forming a substantial endothelial surface layer (ESL) that contributes to the maintenance of endothelial function. As the endothelial glycocalyx is often aberrant *in vitro* and is lost during standard tissue fixation techniques, study of the ESL requires use of intravital microscopy. To best approximate the complex physiology of the alveolar microvasculature, pulmonary intravital imaging is ideally performed on a freely-moving lung. These preparations, however, typically suffer from extensive motion artifact. We demonstrate how closed-chest intravital microscopy of a freely-moving mouse lung can be used to measure glycocalyx integrity via ESL exclusion of fluorescently-labeled high molecular weight dextrans from the endothelial surface. This non-recovery surgical technique, which requires simultaneous brightfield and fluorescent imaging of the mouse lung, allows for longitudinal observation of the subpleural microvasculature without evidence of inducing confounding lung injury.

Video Link

The video component of this article can be found at http://www.jove.com/video/50322/

Introduction

The endothelial glycocalyx is an extracellular layer of proteoglycans and associated glycosaminoglycans lining the vascular intima. *In vivo,* the glycocalyx is highly hydrated, forming a substantial endothelial surface layer (ESL) that regulates a variety of endothelial functions including fluid permeability[1], neutrophil-endothelial adhesion[2], and the mechanotransduction of fluid shear stress[3].

Historically, the glycocalyx has been underappreciated due to its aberrance in cultured cell preparations[4, 5] and its degradation during standard tissue fixation and processing[6]. The increasing use[7] of intravital microscopy (*in vivo* microscopy, IVM) has coincided with heightened scientific interest in the importance of the ESL to vascular function during health and disease. The ESL is invisible to light microscopy and cannot be easily labeled *in vivo*, given the propensity of fluorescent glycocalyx-binding lectins to cause RBC agglutination[8] and fatal pulmonary emboli (unpublished observations). Several indirect approaches have therefore been developed to deduce ESL thickness (and, by extension, glycocalyx integrity) in non-moving vascular beds such as the cremasteric and mesenteric microcirculations. These techniques include the measurement of differences in circulating microparticle velocity as a function of distance from the endothelial membrane (microparticle image velocimetry[9]) as well as the measurement of the exclusion of bulky, fluorescently-labeled vascular markers (*e.g.* dextrans) from the endothelial surface (dextran exclusion technique[10, 11]). Of these techniques, only dextran exclusion is capable of estimating ESL thickness from measurements made at a single point in time. By simultaneously measuring vascular widths using brightfield microscopy (a width inclusive of the "invisible" ESL) and fluorescent microscopy of a vascular tracer excluded from the ESL, ESL thickness can be calculated as one-half the difference between vascular widths[2].

The use of an instantaneous measure of ESL thickness is well-suited for study of the pulmonary glycocalyx. Intravital microscopy of the lung is challenging, given significant pulmonary and cardiac motion artifact. While recent advances allow for immobilization of mouse lungs *in vivo*[12, 13], concerns exist regarding the physiologic impact of lung stasis. Lung immobility is associated with decreased endothelial nitric oxide signaling[14], a signaling pathway that impacts both neutrophil adhesion[15] and lung injury[16]. Furthermore, immobilization of an area of lung exposes surrounding mobile alveoli to injurious shear forces (so-called "atelectrauma"), in accordance with the classic physiologic concepts of alveolar interdependence[17].

In 2008, Arata Tabuchi, Wolfgang Kuebler and colleagues developed a surgical technique allowing for intravital microscopy of a freely-moving mouse lung[18]. Respiratory artifact arising from this technique can be negated by use of high-speed imaging, including simultaneous measurement of brightfield and fluorescent microscopy. In this report, we detail how instantaneous dextran exclusion imaging can be employed to measure ESL thickness in the subpleural microcirculation of a freely-moving, *in vivo* mouse lung. This technique can be easily modified to

determine glycocalyx function-specifically, the ability of an intact ESL to exclude circulating elements from the endothelial surface. We have recently used these techniques to determine the importance of pulmonary ESL integrity to the development of acute lung injury during systemic inflammatory diseases such as sepsis[2].

Protocol

1. Preparation of Surgical Tubing, Vascular Catheters, Chest Wall Window

1. **Intravital microscopy stage.** We custom-made a plexiglass stage upon which the anesthetized mouse lies during microscopy. This stage accommodates both a 15 cm by 10 cm flexible plastic cutting board (upon which the mouse lies during induction of anesthesia, tracheostomy placement, and venous catheterization) as well as a similarly-sized heating element (located underneath the cutting board).
2. **Mouse thoracostomy tube preparation** (**Figure 1**). A 10 cm length of PE 50 tubing (Intramedic, inner diameter 0.58 mm, outer diameter 0.965 mm) is cut. One end is attached to the blunt end of a curved 23 gauge needle; this needle will be used to pass the tube through the thoracic wall (inside → outside) prior to closure of the thoracic window.

   The distal end of the tubing (1.5 cm in length, opposite to the attached 23 gauge needle) is repeatedly punctured by a 30 gauge needle, creating "side ports" to facilitate effective aspiration of intrathoracic air.

   This fenestrated portion is then separated from the rest of the tube by several circumferential loops of 4:0 silk suture; these loops will serve as a "stopper", ultimately anchoring the 1.5 cm fenestrated portion within the chest cavity.
3. **Jugular venous catheters.** Two 15 cm lengths of PE 10 tubing (Intramedic, inner diameter 0.28 mm, outer diameter 0.61 mm) are cut. A scalpel is used to bevel the ends of the tube, thereby increasing the ease of venipuncture. The tubing is flushed via a 1 ml syringe containing 6% 150 kDa dextran solution (in PBS) attached to the non-beveled end of the tubing.
4. **Chest wall window preparation (Figure 2).** Transparent polyvinylidene membrane (New Kure Wrap, Kuresha, Tokyo) is cut into an oval shape (major axis 6 cm, minor axis 4 cm). A circular 5 mm #1 coverslip (Bellco) is affixed to the membrane using α-cyanoacrylate glue (Pattex flüssig, Henkel, Düsseldorf).
5. **Tube for pneumothorax induction ("blow tube").** A 10 cm length of tubing (inner diameter 3 mm, outer diameter 5 mm) is attached to a 5 ml syringe; the opposite end will be used to introduce air into the animal thoracic cage prior to chest wall window engraftment.
6. **Syringe for water immersion of objective.** A 23 gauge needle is attached to a 30 ml syringe containing distilled water. The tip of the needle is blunted (using a metal file) in order to prevent damage to the objective.

2. Mouse Anesthesia

1. A mouse is anesthetized with a mixture of ketamine (10 mg/ml) and xylazine (2 mg/ml), administered intraperitoneally at a dose of 8 µl per gram mouse body weight. Sedation occurs within 3 - 6 min and should not impede spontaneous respiration.
2. Using an electric razor, shave the throat, chest, abdomen, and right side of the mouse.
3. Using tape, secure the mouse to a thin plastic cutting board. The head of the mouse should point towards the operator (**Figure 3**). Gentle tension provided by a loop of suture passing underneath the upper teeth serves to maintain head extension. The cutting board is placed upon a heating pad, maintaining mouse euthermia during tracheostomy and venous catheter placement.
4. Wet shaved areas with 100% ethanol.
5. Confirm adequate anesthesia with a tail/paw pinch. Proceed if minimal response; provide an extra bolus of ketamine/xylazine if not adequately anesthetized.

3. Tracheostomy

1. A 1 cm incision is made over the throat. Underlying connective tissue is dissected, and the salivary glands are separated and reflected laterally. The sternohyoid muscle immediately anterior to the trachea is resected.
2. A loop of 4:0 suture is advanced under the trachea (**Figure 4**). The loop is then cut, creating two separate strands of suture underlying the trachea. The caudal suture will be used to secure the tracheostomy tube; the cranial suture will be used to provide tension on the trachea during tracheostomy placement.
3. Using two fingers, the upper suture is grasped and gentle tension is applied to the trachea. A horizontal incision is made in the trachea between upper and lower sutures. This incision should cross approximately two thirds of the tracheal circumference. A flanged tracheostomy tube (Harvard Apparatus, 1.22 mm outer diameter) is inserted into the distal trachea and secured into place using the caudal tracheal suture.
4. The tracheostomy is connected to a volume-controlled small animal ventilator (Inspira, Harvard Apparatus), and the mouse is ventilated with 40% inspired oxygen and 9 ml/kg tidal volumes (settings optimized to maintain adequate oxygenation/ventilation in our laboratory). Positive end-expiratory pressure (PEEP) is not begun at this point. Of note, ventilator settings should be optimized to unique conditions within individual laboratories. Different lengths of redundant tubing (interposed between the ventilator tubing Y-connector and tracheostomy) can be used to adjust dead space, ensuring stable alveolar ventilation for any chosen tidal volume.

4. Venous Catheterization

1. The junction of the internal and external jugular vein may be identified by tracking distal venous branches proximally. The external jugular is found underneath the reflected salivary glands; this can be traced proximally to find the external-internal jugular junction.
2. Use gentle blunt dissection to separate the jugular junction from surrounding connective tissue.
3. Using 4:0 sutures, tie off the external jugular and internal jugular veins distal (cranial) to the jugular junction.
4. Make a small incision into the carina of the jugular junction; bleeding should be minimal.

5. Two catheters may be incrementally advanced through the incision and into the jugular trunk. After gentle aspiration to ensure blood return, catheters are secured within the vein using 4:0 sutures.
6. Tape venous catheters to the cutting board to prevent against accidental dislodgement.

5. Intravital Mouse Lung Microscopy Surgery (adapted from Tabuchi *et al.*[18])

1. The cutting board (containing the restrained, anesthetized mouse as well as taped venous catheters) is transitioned to the intravital microscopy stage, where the remaining surgical interventions will be performed. A rectal temperature probe is placed; this interfaces with an adaptive heating system (located under the cutting board), allowing maintenance of mouse euthermia.
2. One jugular venous catheter is attached to a syringe pump that delivers a ketamine (10 mg/ml)-xylazine (2 mg/ml) mixture at 200 µl per hour. Adequate anesthesia is again confirmed using tail/paw pinch.
3. The midline incision is extended from the neck to the xyphoid process, then proceeding laterally to the right side (**Figure 5**).
4. Using electrocautery, the chest musculature is removed, exposing the thoracic cage. Care is taken to ensure complete hemostasis.
5. Cross the mouse's right hindleg over the left side and tape down. The resulting abdominal torsion rotates the thorax slightly, improving ease of the surgery.
6. Place the stage at a 45 degree angle (**Figure 6**); this positioning allows the lung to fall away from the chest wall once the pneumothorax is induced.
7. The 1st rib (most inferior rib) is grasped with a forceps and raised; a curved forceps is bluntly pushed underneath the rib. This separates parietal pleura from the chest wall. The pleura should remain unpunctured.
8. Using the blow tube and a syringe, air is forcibly introduced against the parietal pleura. This leads to rupture of the pleural surface and pneumothorax without damaging the underlying lung. The underlying lung will fall away from the chest wall, allowing introduction of an electrocautery forceps without damaging the lung. A decrease in ventilator tidal volume is typically not required during this step.
9. Using electrocautery forceps, dissect the chest wall musculature and cut across the 5th and 6th ribs/parietal pleura, making a ~8 mm circular hole into the chest wall. It is essential that complete hemostasis be maintained, as the presence of bleeding will obscure microscopy (**Figure 7**).
10. Using a needle driver, insert the thoracostomy tube into the chest wall hole. The needle should puncture the chest wall and exit the thoracic cavity inferior and lateral to the thoracic window (**Figure 7**). Take care to avoid puncturing the diaphragm. The tube is then gently pulled out of the chest wall until it resistance occurs from the suture "stopper" located at the edge of the fenestrated portion of the tube.
11. Place the stage flat.
12. Add 3 cm H_2O PEEP to the ventilator to help assist lung reexpansion.
13. Glue (Pattex gel, Henkel) is placed circumferentially around the chest window. The membrane is attached, with the glass cover slip facing exterior to the thoracic cavity. Carefully (and circumferentially) approximate the membrane to the glue using a cotton applicator.
14. While performing a lung recruitment maneuver (3 tidal volumes during which the PEEP ventilator port is obstructed), -3 mm Hg suction is applied to the chest tube. The lung should persistently approximate the membrane while freely moving during tidal ventilation (**Figure 8**).
15. The right foreleg of the mouse is crossed over to the left side, resulting in a left lateral decubitus position of the mouse. Sponge wedges can be used to properly position the mouse so the chest window is aligned with the microscopy water immersion objective.
16. Distilled water is placed on the cover slip prior to microscopy, allowing for visualization of the lung using a water immersion objective. Water will need to be intermittently replenished throughout imaging.

6. Measurement of the Pulmonary Endothelial Surface Layer Thickness

1. Immediately after chest wall closure, 500 µl FITC-labeled 150 kDa dextran (6% solution in PBS) is administered via the second (non-anesthesia) jugular venous catheter. This bolus serves as volume resuscitation as well as the vascular tracer for ESL measurement. The dextran bolus does not influence neutrophil adhesion or lung edema formation[2].
2. The water immersion objective is centered over the cover slip. The choice of objective is essential-to visualize small differences in ESL thickness, a high numerical aperture is needed (> 0.8) while still maintaining a 2 - 3 mm working distance (allowing penetration through the lung window and pleural surface). We use the Nikon CFI 75 LWD 16x (NA 0.8) and CFI 75 LWD 25x (NA 1.1) objectives for this purpose.
3. To accurately measure ESL thickness in a moving organ, it is essential that brightfield and fluorescent vascular widths are performed simultaneously. This may be accomplished using an image splitter (Dual View, Photometrics) that allows for simultaneous capture of reflected light differential interference contrast (DIC, brightfield) and FITC images (**Figure 9**).
4. During a 5 sec inspiratory pause, continuous imaging is performed and recorded. Later, these images may be reviewed to identify in-focus frames.
5. Using an in-focus frame, subpleural microvessels (< 20 µm diameter) are identified; at least 3 microvessels are typically found on a single frame. After completion of the experiment, DIC and FITC-dextran vascular widths are measured (by a blinded observer) by averaging the lengths of three perpendicular intercepts per microvessel. Assuming equal ESL thickness at both edges of the vessel, the ESL size can be defined by one-half the difference between DIC and FITC-dextran vascular widths, as described in the Representative Results section.
6. Typically, intravital microscopy can be performed for > 90 min without any evidence of lung injury or hypotension[2]. Preliminary experiments should be performed to confirm mouse stability (blood pressure, oxygenation, ventilation, lung injury) during the period of observation. Experimental drugs may be introduced through the second (non-anesthetic) jugular catheter at any point during the procedure.

7. Alternative Measurement of the Pulmonary Endothelial Surface Layer Integrity

The intact endothelial surface layer functions (in part) to exclude circulating elements from the endothelial surface[2]. ESL integrity can therefore be measured by the ability of a circulating element (*e.g.* a fluorescent microsphere) to access and interact with cell surface adhesion molecules (such as ICAM-1).

1. Anti-ICAM-1 labeled fluorescent microspheres are prepared prior to surgery. Streptavidin-coated 0.97 µm fluorescent microspheres are incubated with biotinylated anti-ICAM-1 (YN1/1.7.4 clone, 1:50, eBioscience) antibody or isotype control for 30 min at room temperature. The microspheres are washed thrice and suspended in PBS at 1 x 10^9 microspheres per ml.
2. During intravital microscopy, the microsphere suspension (100 µl) is injected into the jugular venous catheter. After 15 min of circulation, fluorescent images are captured over 5 min. Microspheres immobile for > 5 min are considered adherent and quantified using image processing software.

8. Euthanasia

After completion of the procedure, anesthetized mice are euthanized by exsanguination via direct cardiac puncture. Euthanasia is confirmed via bilateral pneumothoraces, after which lungs are harvested and snap-frozen for later analysis.

Representative Results

The experimental approach described in steps 1-6 will allow capture of multiple frames of simultaneous DIC (brightfield) and fluorescent images. To determine ESL thickness, recorded images are reviewed by a blinded observer after completion of the experimental protocol. Using an in-focus frame, subpleural microvessels (< 20 µm diameter) are identified; at least 3 microvessels are typically found on a single frame (**Figure 10**). Using image analysis software (NIS Elements, Nikon), vascular widths are measured (by a blinded observer) by averaging the lengths of three perpendicular intercepts per microvessel. As the ESL is invisible to DIC imaging, DIC vascular widths span endothelial membrane to endothelial membrane and are therefore inclusive of ESL thickness[9, 10]. In contrast, FITC-dextran (150 kDa) is excluded from the ESL. Consequently, FITC vascular widths do not incorporate ESL thickness. Assuming equal ESL thickness at both edges of the vessel, the ESL size can therefore be defined by one-half the difference between DIC and FITC-dextran vascular widths.

Several potential technical pitfalls may interfere with interpretation of experimental results. The presence of bleeding into the microscopy field will obscure both DIC and FITC visualization of the subpleural microvasculature; therefore, care must be taken to obtain hemostasis (using electrocautery) during window placement (5.9). Additionally, the lung might not reapproximate the thoracic window after the recruitment maneuver (5.14); this usually indicates incomplete circumferential adhesion of the membrane around the thoracic window. This can usually be corrected by reapplication of glue around the thoracic window, followed by a repeat lung recruitment maneuver. Finally, care must be taken to avoid accidental injection of intravenous air into the mouse. Air emboli, even if not fatal, will preferentially travel to the nondependent lung, preventing FITC-dextran perfusion of the visualized (nondependent) subpleural microvasculature.

Measurement of ESL widths requires use of an image splitter (affording simultaneous DIC and fluorescent imaging) as well as specialized microscopy objectives. These equipment demands may be avoided with some modifications to our protocol. Glycocalyx integrity may be indirectly measured by determining ESL exclusion of circulating microspheres from the vessel surface. The presence of ESL degradation, therefore, is indicated by increased subpleural microvascular capture of microspheres targeted against endothelial surface adhesion molecules (such as ICAM-1) (**Figure 11**).

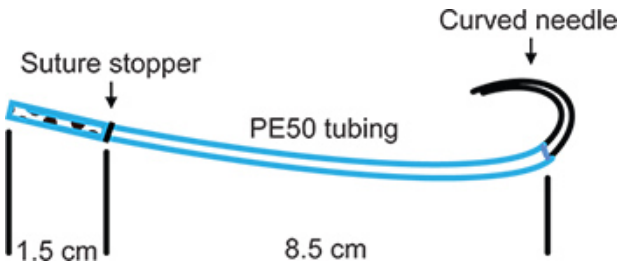

Figure 1.

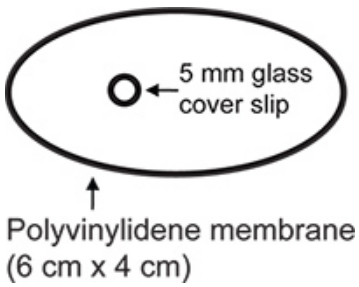

Figure 2.

Figure 3.

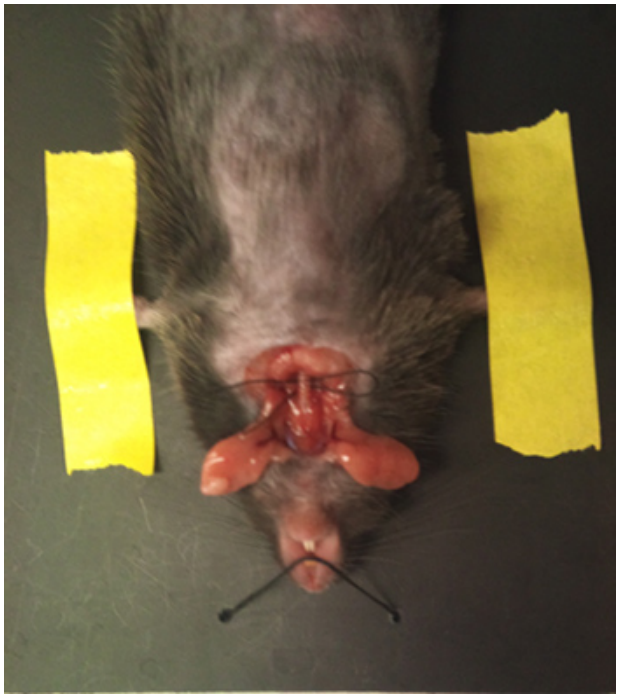

Figure 4.

Figure 5.

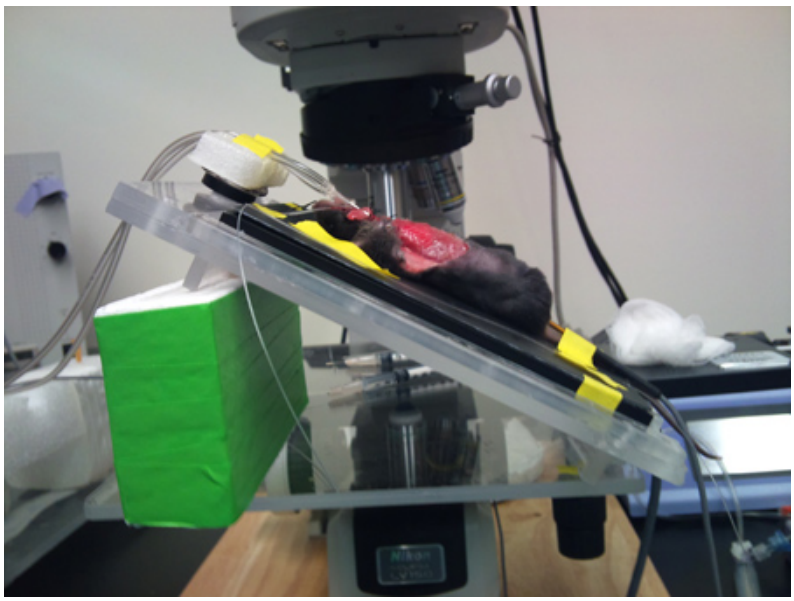

Figure 6.

Figure 7.

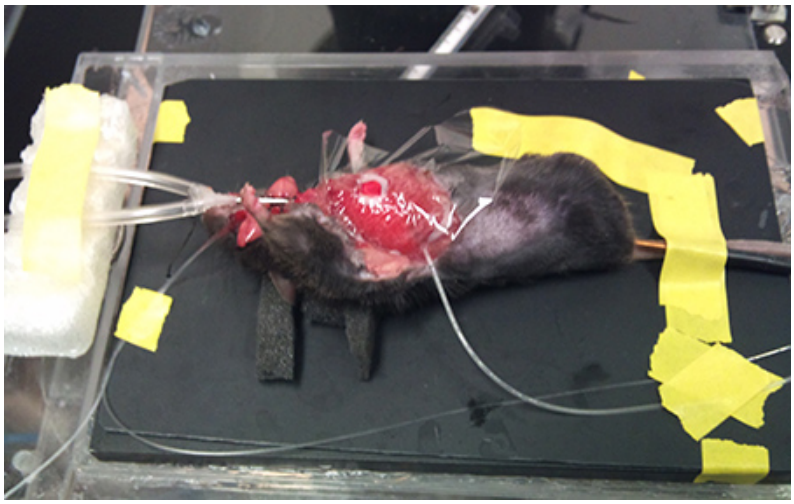

Figure 8.

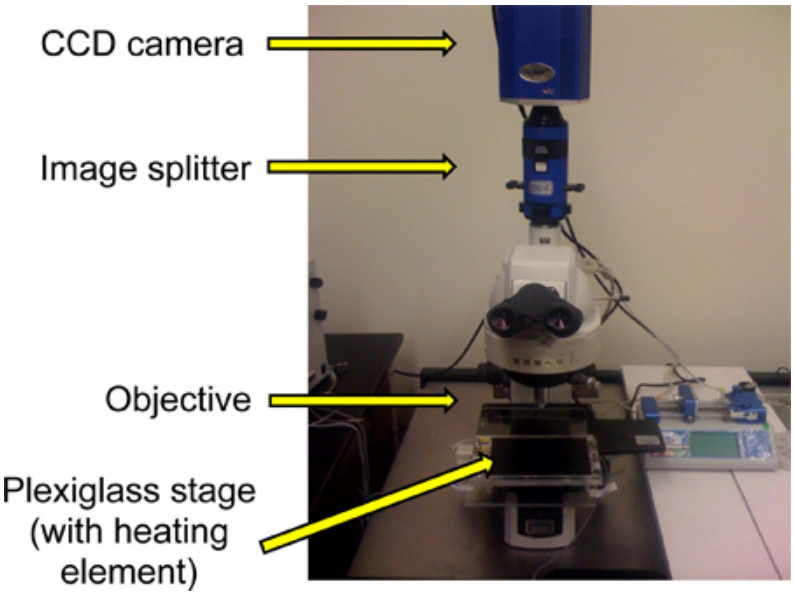

Figure 9.

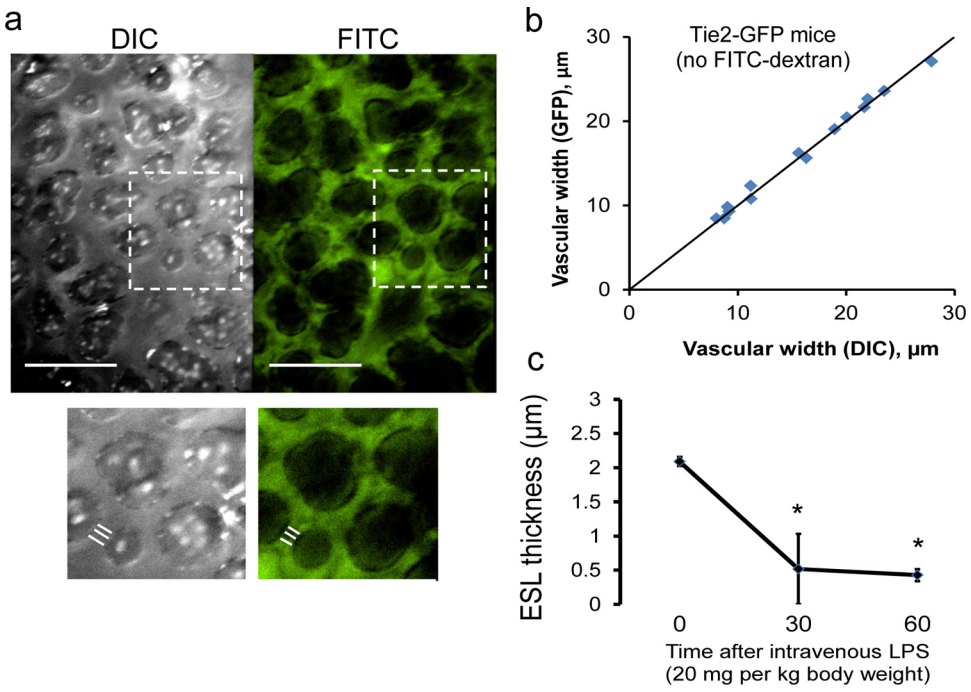

Figure 10. Measurement of mouse pulmonary ESL thickness**. (a)** Representative simultaneously-captured DIC and fluorescent images of the mouse subpleural microvasculature (scale bar, 50 µm). Microvessel width is measured using the average of three perpendicular linear intercepts. ESL thickness can be determined by one-half the difference between DIC (inclusive of the ESL) and fluorescent (exclusive of the ESL) microvessel widths. **(b)** DIC measurements accurately identify subpleural vessel wall borders, as demonstrated by nearly-identical DIC and GFP vessel width measurements performed in endothelial-fluorescent Tie2-GFP mice (Jackson Labs). Solid line represents line of identity. **(c)** The subpleural microvasculature can be followed longitudinally, as evidenced by the progressive loss of ESL thickness occurring after intravenous lipopolysaccharide (LPS). *n* = 3 mice. * *P* < 0.05 in comparison to time = 0 min by ANOVA.

Movie 1. Glycocalyx integrity can be determined by assessing for anti-ICAM-1 microsphere adherence within the subpleural microvasculature. High-speed confocal microscopy (Nikon A1R) demonstrates adherent fluorescent microspheres 45 min after intravenous LPS (20 mg per kg body weight). Note that circulating microspheres can be occasionally seen passing through the microcirculation. To improve visualization of (green fluorescent) microsphere localization, in step 6.1 mice were pretreated with the vascular tracer TRITC-dextran (150 kDa, 6%) in lieu of FITC-dextran. Click here to view movie.

Discussion

Coincident with the expanding use of *in vivo* microscopy, there is increasing appreciation for both the substantial size of the ESL as well as its numerous contributions to vascular function. These emerging data, however, are primarily derived from studies of the systemic vasculature. Indeed, use of *in vivo* microscopy in the lung is technically challenging, given significant pulmonary and cardiac motion artifact.

Several recent technical advances have allowed for stabilization of the moving mouse lung, affording better application of intravital techniques to the pulmonary microcirculation[12, 13]. These approaches, however, are potentially confounded by the physiologic ramifications of lung immobility. As the lung is teleologically an organ intended for continuous motion, lung stasis will intuitively alter pulmonary physiology. Indeed, lung stasis is associated with alterations in endothelial nitric oxide signaling, a pathway with numerous downstream consequences in both the healthy and injured lung[14, 16]. Furthermore, immobilization of one area of the lung subjects surrounding alveoli to injurious shear forces, consistent with the "atelectrauma" characteristic of ventilator induce lung injury[19]. These and other yet-to-be-identified consequences of lung stasis are likely to confound interpretation of intravital observations of pulmonary microvascular (patho)physiology.

Given these concerns, we sought to develop a method by which the pulmonary ESL could be studied in a freely moving, *in vivo* mouse lung. We chose to adapt the technique of Tabuchi and Kuebler, an approach that allows longitudinal visualization of a freely-moving mouse lung without inciting pulmonary injury[18]. Importantly, our approach contains several subtle alterations from Tabuchi's original protocol; these alterations evolved from the need to accommodate unique conditions within our laboratory. Similarly, adoption of our model of ESL measurement elsewhere will require similar optimization to ensure the stability of mouse hemodynamics, oxygenation, ventilation, and the absence of lung injury.

We chose to use dextran exclusion as our primary approach to ESL measurement. This technique is well-suited for our model, as ESL measurements can be made from a single moment in time, negating pulmonary and cardiac motion artifact. While previous studies of the systemic microvasculature have suggested that dextran exclusion is only accurate in small vessels (< 15 µm[6]), we have noted concordant ESL changes in vessels up to 30 µm of diameter. These discrepancies may be due to optical characteristics specific to the pleural surface.

In a moving vascular bed, it is essential that brightfield and fluorescent imaging occurs simultaneously, as even a brief delay in image acquisition (*e.g.* shutter closure between sequential images) would fatally confound measurements of ESL thickness. While pausing ventilation may decrease this confounding, an inspiratory pause will not completely prevent cardiac motion artifact or respiratory artifact from gas redistribution in heterogeneously-inflated, injured lungs ("pendelluft")[20]. We elected to use an image splitter to simultaneously send brightfield and fluorescent images to a single CCD camera. Alternative approaches could potentially include the use of dichroic mirrors to simultaneously capture reflected light and fluorescent images during confocal microscopy.

An additional critical demand of our model is the use of specialized water-immersion objectives. These objectives must have a sufficiently large numerical aperture to allow resolution of small differences in vessel widths while still maintaining an adequate working distance to penetrate both the thoracic window and pleural surface. These objectives, while available, are highly expensive. The use of reflected light differential interference contrast (DIC) microscopy, a brightfield technique that highlights unstained tissue edges, is additionally desirable, as DIC improves precision of vascular width measurements.

Alternative techniques exist for the determination of pulmonary ESL width. While microsphere velocimetry cannot be accurately performed on a moving vascular bed, microsphere adhesion can be employed to indirectly test pulmonary glycocalyx integrity. We have previously shown that the intact ESL functions to exclude circulating microspheres from endothelial surface adhesion molecules[2]. The presence of anti-ICAM-1 microsphere adhesion to the endothelial surface therefore indicates a loss of glycocalyx/ESL integrity. This technique does not require simultaneous brightfield/fluorescent imaging, nor are high numerical aperture objectives necessary. However, one important caveat exists: for increased anti-ICAM-1 microsphere adhesion to indicate glycocalyx loss, there must be similar ICAM-1 cell surface expression between control and experimental groups. While ICAM-1 endothelial surface expression remained stable early (< 45 min) in sepsis-induced lung injury[2], surface expression will eventually increase in a NF-κB dependent manner[21]. Use of microsphere adhesion as a marker of glycocalyx integrity, therefore, may only be valid during early inflammation.

Of note, while our surgical and microscopy techniques do not induce lung injury[2], it is uncertain how evolving experimental lung injury (*e.g.* injury induced by intratracheal acid instillation) influences measurements of ESL thickness. Evolving lung edema could potentially confound DIC measurements of vessel width and/or influence dextran permeability. This uncertainty can be mitigated by the complementary use of multiple techniques (*e.g.* dextran exclusion, microsphere adhesion, as well as confirmatory histologic assessments of vessel glycosaminoglycan content[2]) to confirm observed changes in the pulmonary ESL.

In summary, by expanding the surgical approach initially reported by Tabuchi and Kuebler, we have developed an experimental model that allows for the detailed observation of the pulmonary ESL. Use of this model should allow for a greater understanding of the importance of the endothelial glycocalyx to pulmonary vascular physiology in health and disease.

Disclosures

No conflicts of interest declared.

Acknowledgements

We thank Drs. Arata Tabuchi and Wolfgang Kuebler (University of Toronto) for instruction regarding intravital microscopy. We thank Andrew Cahill (Nikon Instruments) for assistance in microscopy design and implementation. This work was funded by NIH/NHLBI grants P30 HL101295 and K08 HL105538 (to E.P.S.).

References

1. Negrini, D.,Tenstad, O., Passi, A., & Wiig, H. Differential degradation of matrix proteoglycans and edema development in rabbit lung. *AJP - Lung Cellular and Molecular Physiology*. **290**, L470-L477 (2006).
2. Schmidt, E.P., *et al.* The pulmonary endothelial glycocalyx regulates neutrophil adhesion and lung injury during experimental sepsis. *Nat. Med*. **18**, 1217-1223 (2012).
3. Florian, J.A., *et al.* Heparan sulfate proteoglycan is a mechanosensor on endothelial cells. *Circ. Res.* **93**, e136-e142 (2003).
4. Chappell, D., *et al.* The Glycocalyx of the Human Umbilical Vein Endothelial Cell: An Impressive Structure *Ex Vivo* but Not in Culture. *Circulation Research*. **104**, 1313-1317 (2009).
5. Potter, D.R. & Damiano, E.R. The hydrodynamically relevant endothelial cell glycocalyx observed *in vivo* is absent *in vitro. Circ. Res.* **102**, 770-776 (2008).
6. Weinbaum, S.,Tarbell, J.M., & Damiano, E.R. The Structure and Function of the Endothelial Glycocalyx Layer. *Annual Review of Biomedical Engineering*. **9**, 121-167 (2007).
7. Pittet, M. & Weissleder, R. Intravital Imaging. *Cell*. **147**, 983-991 (2011).
8. Kilpatrick, D.C., Graham, C.,Urbaniak, S.J., Jeffree, C.E., & Allen, A.K. A comparison of tomato (Lycopersicon esculentum) lectin with its deglycosylated derivative. *Biochem. J*. **220**, 843-847 (1984).
9. Smith, M.L., Long, D.S., Damiano, E.R., & Ley, K. Near-wall micro-PIV reveals a hydrodynamically relevant endothelial surface layer in venules *in vivo. Biophys. J*. **85**, 637-645 (2003).
10. Vink, H. & Duling, B.R. Identification of Distinct Luminal Domains for Macromolecules, Erythrocytes, and Leukocytes Within Mammalian Capillaries. *Circ. Res*. **79**, 581-589 (1996).
11. Marechal, X., *et al.* Endothelial glycocalyx damage during endotoxemia coincides with microcirculatory dysfunction and vascular oxidative stress. *Shock*. **29**, 572-576 (2008).

12. Presson Jr, R.G., *et al.* Two-Photon Imaging within the Murine Thorax without Respiratory and Cardiac Motion Artifact. *The American Journal of Pathology*. **179**, 75-82 (2011).
13. Looney, M.R,. *et al.* Stabilized imaging of immune surveillance in the mouse lung. *Nat. Meth.* **8**, 91-96 (2011).
14. Pearse, D.B., Wagner, E.M., & Permutt, S. Effect of ventilation on vascular permeability and cyclic nucleotide concentrations in ischemic sheep lungs. *J. Appl. Physiol*. **86**, 123-132 (1999).
15. Hossain, M., Qadri, S., & Liu, L. Inhibition of nitric oxide synthesis enhances leukocyte rolling and adhesion in human microvasculature. *Journal of Inflammation*. **9**, 28 (2012).
16. Schmidt, E.P., *et al.* Soluble guanylyl cyclase contributes to ventilator-induced lung injury in mice. *AJP - Lung Cellular and Molecular Physiology.* **295**, L1056-L1065 (2008).
17. Mead, J., Takishima, T., & Leith, D. Stress distribution in lungs: a model of pulmonary elasticity. *J. Appl. Physiol*. **28**, 596-608 (1970).
18. Tabuchi, A., Mertens, M., Kuppe, H., Pries, A.R., & Kuebler, W.M. Intravital microscopy of the murine pulmonary microcirculation. *J. Appl. Physiol.* **104**, 338-346 (2008).
19. Gattinoni, L., Protti, A., Caironi, P., & Carlesso, E. Ventilator-induced lung injury: the anatomical and physiological framework. *Crit. Care Med*. **38**, S539-S548 (2010).
20. Tabuchi, A., Kim, M., Semple JW., & Kuebler, WM. Acute Lung Injury Causes Pendelluft Between Adjacent Alveoli *In Vivo. Am. J. Respir. Crit. Care Med.* **183**, A2490 (2011).
21. Roebuck, K.A. & Finnegan, A. Regulation of intercellular adhesion molecule-1 (CD54) gene expression. *J. Leukoc. Biol.* **66**, 876-888 (1999).

